View metadata, citation and similar papers at core.ac.uk

brought to you by CORE

provided by Tamkang University Institutional Repository

AIP Journal of Applied Physics

Effect of Ga doping on charge transport mechanism of La 0.85 Zr 0.15 Mn 1 − x Ga x O 3

D. C. Ling, J. H. Cheng, C. L. Lee, and F. Z. Chien

Citation: Journal of Applied Physics **105**, 07D723 (2009); doi: 10.1063/1.3073950

View online: http://dx.doi.org/10.1063/1.3073950

View Table of Contents: http://scitation.aip.org/content/aip/journal/jap/105/7?ver=pdfcov

Published by the AIP Publishing

Articles you may be interested in

Influences of the first-to-second order magnetic phase transformation on the transport properties of La0.7Ca0.3−xBaxMnO3 compounds
J. Appl. Phys. **115**, 17C706 (2014); 10.1063/1.4860943

Magnetic transitions and electrical transport in Bi-doped lanthanum strontium manganites
Low Temp. Phys. **40**, 418 (2014); 10.1063/1.4876222

ac susceptibility studies in Fe doped La 0.65 Ca 0.35 Mn 1 − x Fe x O 3 : Rare earth manganites
J. Appl. Phys. **108**, 113907 (2010); 10.1063/1.3517113

Thermopower and thermal conductivity of the electron-doped manganite La 0.9 Te 0.1 Mn O 3
J. Appl. Phys. **100**, 123701 (2006); 10.1063/1.2402030

Transport mechanism and magnetothermoelectric power of electron-doped manganites La 0.85 Te 0.15 Mn 1 − x Cu x O 3 (0 x 0.20)
J. Appl. Phys. **100**, 073706 (2006); 10.1063/1.2356106

2014 Special Topics

PEROVSKITES

2D MATERIALS

MESOPOROUS MATERIALS

BIOMATERIALS/ BIOELECTRONICS

METAL-ORGANIC FRAMEWORK MATERIALS

AIP APL Materials

Submit Today!

[This article is copyrighted as indicated in the article. Reuse of AIP content is subject to the terms at: http://scitation.aip.org/termsconditions. Downloaded to] IP: 163.13.36.187 On: Mon, 20 Oct 2014 01:56:55

Effect of Ga doping on charge transport mechanism of $La_{0.85}Zr_{0.15}Mn_{1-x}Ga_xO_3$

D. C. Ling,[a] J. H. Cheng, C. L. Lee, and F. Z. Chien
Department of Physics, Tamkang University, Tamsui 25137, Taiwan

(Presented 12 November 2008; received 22 September 2008; accepted 4 December 2008; published online 18 March 2009)

Structural properties, temperature-dependent resistivity $\rho(T)$ and thermoelectric power $S(T)$ of $La_{0.85}Zr_{0.15}Mn_{1-x}Ga_xO_3$ (LZMGO) manganites with $0.0 \leq x \leq 0.06$ have been extensively investigated. It is found that the Mn–O–Mn bond angle decreases and the Mn–O bond length increases with increasing Ga content, indicative of a significant distortion of MnO_6 octahedra in LZMGO. The local lattice distortion and suppression of double exchange ferromagnetism induced by the Ga doping shift both Curie temperature (T_C) and metal-insulator transition temperature (T_{MI}) toward lower temperatures. Followed by the metal-insulator transition, $\rho(T)$ exhibits an insulatinglike behavior accompanied by a relatively small value of $S(T)$ below T^* at low temperatures. An anomalous peak observed in $S(T)$ is attributed to an enhancement of electron-magnon interaction caused by the Ga doping and a decrease in magnetic entropy near T_{MI}. Three different charge transport mechanisms were identified in three temperature regions based on detailed analyses of $\rho(T)$ and $S(T)$ data. The small-polaron hopping mechanism governs the charge transport in the high-temperature paramagnetic region ($T > T_{MI}$). The polaron binding energy determined from the $\rho(T)$ and $S(T)$ data increases with increasing Ga content, suggesting that polaron in $La_{0.85}Zr_{0.15}MnO_3$ has a magnetic nature. In addition, the electron-magnon scattering dominates the charge transport in the intermediate-temperature metallic region ($T^* < T < T_{MI}$), whereas the transport behavior in the low-temperature insulating region ($T < T^*$) can be described by the three-dimensional variable-range-hopping model. © *2009 American Institute of Physics*. [DOI: 10.1063/1.3073950]

Electron-doped manganites $La_{1-x}A_xMnO_3$ (A = Ce, Te, Zr) have stimulated considerable scientific interest on account of the colossal magnetoresistance (CMR) and the potential applications in spintronics.[1–3] It has been shown experimentally that the valence state of Mn in the $La_{1-x}A_xMnO_3$ is indeed a mixed valence of Mn^{2+} and Mn^{3+}.[4–6] Therefore, the hopping of itinerant e_g^2 electron mediated by double exchange (DE) interaction via $Mn^{3+}-O-Mn^{2+}$ network is expected to be an essential ingredient of the CMR effect in the electron-doped manganites. More recently, Ling *et al.*[7] demonstrated that the DE mechanism is responsible for charge transport in $La_{0.85}Zr_{0.15}MnO_3$. Despite extensive studies,[1–7] the interplay between the CMR effect and other factors such as Jahn–Teller (JT) effect, polaron formation, and charge/orbital ordering in the electron-doped manganites is still lacking. It is believed that the study of the Mn-site substitution should provide important information about the mechanism of the CMR behavior because of the crucial role of Mn ions. Among the investigations of all the Mn-site substitution, the Ga doping at the Mn site is strategically interesting because Ga^{3+} has no magnetic moment and ionic size of Ga^{3+} (0.62 Å) is slightly smaller than that of Mn^{3+} (0.65 Å). Thus, static lattice effects and any additional magnetic exchange interactions are not introduced by the Ga doping.[8] To shed light on a better understanding of the transport mechanism of $La_{0.85}Zr_{0.15}MnO_3$, we have performed thermoelectric power (TEP) measurements on $La_{0.85}Zr_{0.15}Mn_{1-x}Ga_xO_3$ with $0.0 \leq x \leq 0.06$ in addition to the basic characterization by resistivity and magnetization measurements. We will show that the *local* lattice distortion in MnO_6 octahedra and random dilution of the Mn sublattice induced by the Ga doping have a significant impact on charge transport in $La_{0.85}Zr_{0.15}Mn_{1-x}Ga_xO_3$.

The samples investigated were prepared by the solid-state reaction method. The detailed synthesis process will be published elsewhere. The structure and phase purity of the samples were characterized by x-ray powder diffraction (XRD) patterns. The $\rho(T)$ and $S(T)$ measurements were done with physical property measurement system (PPMS).

Figure 1 shows the observed, the refined, and the difference XRD patterns for LZMGO with $x=0.04$ at room temperature. All Bragg peaks can be indexed with a rhombohedral lattice of space group $R\bar{3}C$. Other LZMGO samples studied also exhibit single-phase XRD patterns. Studying LZMO with Ga content up to only 0.06 is due to the fact that LZMGO with Ga content larger than 0.06 is not hard enough to place contact leads on. The structural parameters obtained from Rietveld refinement for samples investigated are listed in Table I. The a- and c-axis lattice constants and the Mn–O–Mn bond angle monotonically decrease with increasing Ga content arising from the chemical-pressure-induced distortion of MnO_6 octahedra in LZMGO. Both room-temperature resistivity and Mn–O bond length follow a simi-

[a]Author to whom correspondence should be addressed. Electronic mail: dcling@mail.tku.edu.tw.

 © 2009 American Institute of Physics

[This article is copyrighted as indicated in the article. Reuse of AIP content is subject to the terms at: http://scitation.aip.org/termsconditions. Downloaded to] IP: 163.13.36.187 On: Mon, 20 Oct 2014 01:56:55

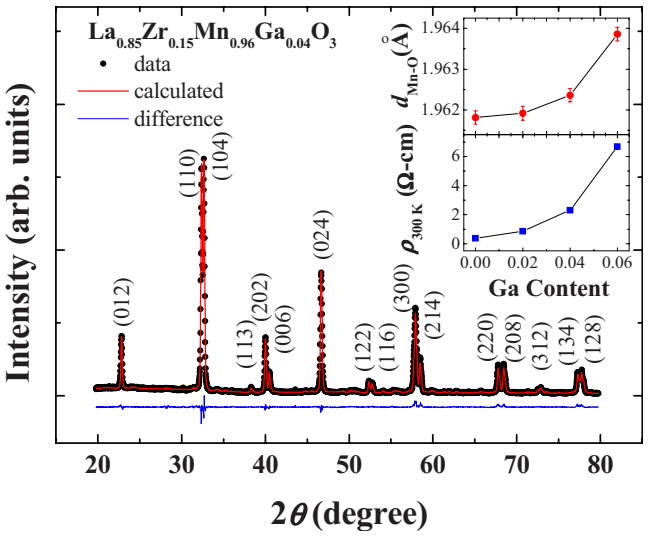

FIG. 1. (Color online) Observed, refined, and difference XRD patterns for $La_{0.85}Zr_{0.15}Mn_{0.96}Ga_{0.04}O_3$. $\rho_{300\ K}$ and Mn–O bond length as a function of Ga content are displayed in the inset.

lar Ga-content dependence displayed in the inset of Fig. 1, indicating that the local lattice distortion of MnO_6 is intimately related to charge transport of LZMGO in high-temperature paramagnetic region.

In addition, the nonmagnetic Ga^{3+} doping would introduce random dilution in the Mn sublattice and suppress the dynamic JT distortion. As a result, it weakens local DE interaction and shifts both T_{MI} and T_C toward low temperatures with increasing Ga content, as illustrated in Fig. 2(a) and the inset of Fig. 2(b), respectively. Similar to the observed results in the hole-doped manganites, a gradual decrease in the zero-field-cooled (ZFC) magnetization below T_C and a discrepancy between M_{ZFC} and M_{FC} at low temperatures likely arise from the canted nature of spins or the random freezing of spins.[9,10] $\rho(T)$ exhibits an insulatinglike behavior with $d\rho/dT<0$ below T^*, increasing from 23 K for $x=0$ to 49 K for $x=0.06$, and comes with an increase in resistivity by four orders of magnitude at 2 K. It could be due to carrier localization subjected to the random potential at the Mn site and the growth of spin-glass-like clusters caused by the Ga doping at low temperatures. TEP as a function of temperature for LZMGO reveals an anomalous peak and accompanies a relatively small value below T^*, as displayed in Fig. 2(b). The Ga-doping-dependent peak observed in TEP is probably attributed to an enhancement of magnon drag associated with electron-magnon interaction and a decrease in magnetic entropy near T_{MI}.

TABLE I. Refined structural parameters for $La_{0.85}Zr_{0.15}Mn_{1-x}Ga_xO_3$.

	$x=0.00$	$x=0.02$	$x=0.04$	$x=0.06$
a (Å)	5.5228(6)	5.5141(3)	5.5103(6)	5.5092(5)
c (Å)	13.3574(6)	13.3426(8)	13.3377(1)	13.3342(2)
Mn–O (Å)	1.9618(2)	1.9619(2)	1.9623(6)	1.9638(8)
Mn–O–Mn (deg)	164.529(4)	163.524(1)	162.771(2)	162.164(1)
x (O)	0.5478(2)	0.5509(8)	0.5540(2)	0.5552(5)
R_{WP} (%)	5.36	5.68	5.27	5.57

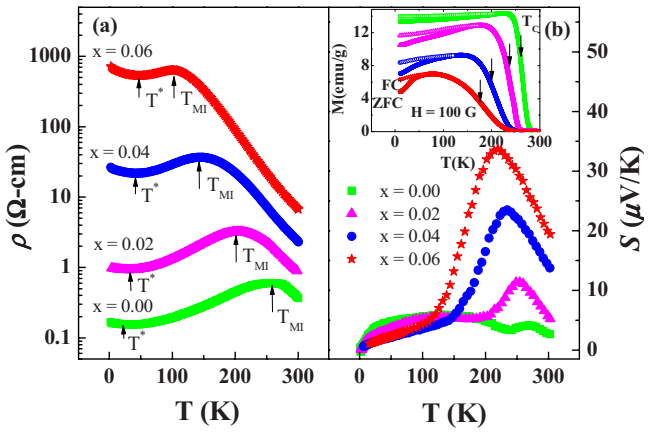

FIG. 2. (Color online) (a) $\rho(T)$ and (b) $S(T)$ for LZMGO. $M_{ZFC}(T)$ and $M_{FC}(T)$ for LZMGO in a field of 100 G are shown in the inset of (b). T_{MI}, T^*, and T_C are indicated by arrows.

In the high-temperature insulating region of $T>T_{MI}$, $\ln(\rho/T)$ and S versus T^{-1} for LZMGO are plotted in Figs. 3(a) and 3(b), respectively. It is clear that experimental data fit to straight lines very well, indicative of a strong support of the adiabatic small-polaron hopping (SPH) model with $\rho(T)=BT\exp(E_p/k_BT)$ and $S(T)=k_B/e(E_s/k_BT+\alpha)$, where E_p is the polaron hopping energy, E_s is the activation energy needed to produce a stationary number of carriers, and α is a constant associated with the sum of the spin entropy and the charge-carrier entropy.[11,12] The resistivity coefficient B is expressed by $2k_B/3ne^2a^2\nu$, where n is the polaron concentration, e is the electronic charge, a is the hopping distance, and ν is the frequency of the longitudinal optical phonons.[13] The fitted parameters B, E_p, and E_s summarized in Table II are found to increase with increasing Ga content. The comparatively large difference between the obtained E_p and E_s is a signature of SPH wherein the transport is dominated by temperature-dependent mobility effects.[14] It seems unlikely that either a or ν changes sufficiently to account for the large

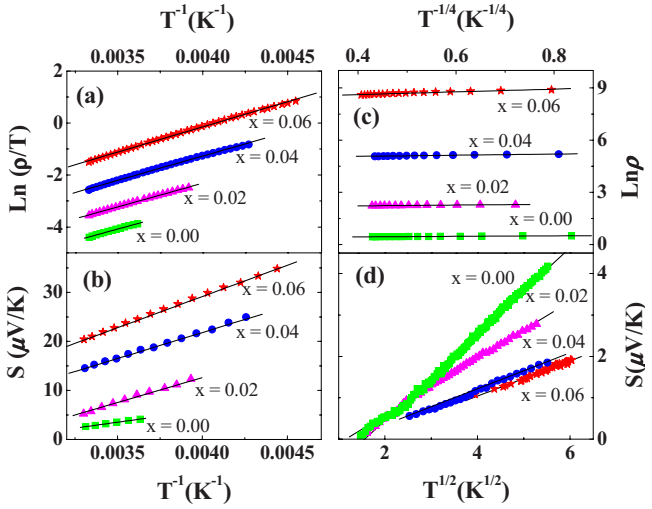

FIG. 3. (Color online) (a) $\ln(\rho/T)$ and (b) S are plotted against T^{-1} for LZMGO in the high-temperature paramagnetic region. The solid lines are the fit to the SPH model. (c) $\ln\rho$ vs $T^{-1/4}$ and (d) S vs $T^{1/2}$ for LZMGO in the low-temperature insulating region. The solid lines represent the fit to the 3D VRH model.

[This article is copyrighted as indicated in the article. Reuse of AIP content is subject to the terms at: http://scitation.aip.org/termsconditions. Downloaded to] IP: 163.13.36.187 On: Mon, 20 Oct 2014 01:56:55

TABLE II. Transport parameters for LZMGO.

Ga content	B (10^{-4} Ω cm/K)	E_s (meV)	E_p (meV)
$x=0.00$	2.514	4.75	150.42
$x=0.02$	5.421	8.15	155.49
$x=0.04$	14.923	10.62	161.11
$x=0.06$	34.466	12.75	169.34

increase in B as the Ga content increases. Therefore, it is reasonable to speculate that a reduction in n arising from a decrease in JT ions Mn^{3+} caused by Ga^{3+} doping is responsible for the large increase in B. Moreover, the deduced activation energy E_p gradually increases with increasing Ga content, indicating that the local lattice distortion induced by the Ga doping lifts the degeneracy of the e_g state of Mn ion. As a result, the lower e_g state serves as a trapping level and gives rise to a higher energy barrier for the polaron to hop over. The polaron binding energy determined from $E_b=2(E_p-E_s)$ increases from 291 to 313 meV as the Mn^{3+} content decreases from 1.00 to 0.94, in strong contrast to the results reported in $La_{1-y}Ca_yMnO_3$,[15] suggesting that the local lattice distortion and suppression of local DE ferromagnetism induced by the Ga doping are predominately responsible for the formation of the polaron in LZMGO. This finding provides strong evidence for the existence of magnetic nature of polaron in $La_{0.85}Zr_{0.15}MnO_3$.

In the intermediate-temperature metallic region of $T^*<T<T_{MI}$, $\rho(T)$ and $S(T)$ can be best fitted by $\rho(T)=\rho_0+\rho_{2.5}T^{2.5}$ and $S(T)=S_0+S_{1.5}T^{1.5}+S_4T^4$, respectively, where ρ_0 is a T-independent resistivity related to domain, grain boundary, and other T-independent scattering mechanisms,[16,17] the $\rho_{2.5}T^{2.5}$ term is attributed to electron-magnon scattering process,[17,18] the $S_{1.5}T^{1.5}$ term accounts for magnon drag effect,[19] and the S_4T^4 term may be due to the spin-wave fluctuation in the ferromagnetic phase.[19,20] It is found that the value of the fitted parameter ρ_0 increases from 6.45×10^{-2} to 4.73×10^{2} Ω cm and that of $\rho_{2.5}$ varies from 1.32×10^{-5} to 1.83×10^{-2} Ω cm/$K^{2.5}$ as x increases from 0.00 to 0.06, indicating that the Ga doping results in the enhancement of the domain or grain boundary scattering and significantly increases the electron-magnon scattering in the $T^*<T<T_{MI}$ region. In addition, the value of $S_{1.5}$ is seven orders of magnitude larger than that of S_4, suggesting that the $S_{1.5}T^{1.5}$ term dominates the transport mechanism in the ferromagnetic metallic region below T_{MI}. It should be noted that $S_{1.5}$ associated with magnon drag effect is approximately proportional to the magnon specific heat $C_m=4.45k_B^{5/2}/4\pi^2D^{3/2}$, where D is the spin-wave stiffness.[21,22] Therefore, the increase in $S_{1.5}$ from 1.23×10^{-2} μV/$K^{5/2}$ for $x=0.00$ to 4.53×10^{-2} μV/$K^{5/2}$ for $x=0.06$ corresponds to a reduction in the spin-wave stiffness. Consequently, it leads to a significant enhancement of electron-magnon scattering manifesting itself as a remarkable increase in $\rho_{2.5}$ mentioned above.

In the low-temperature insulating region of $T<T^*$, the carrier transport behavior follows Mott's three-dimensional (3D) variable-range-hopping (VRH) model with expression $\rho\propto\exp[(T_0/T)^{1/4}]$, as shown in Fig. 3(c), where $T_0\propto1/\zeta^3$, and ζ is the localization length.[23] The fitting parameter T_0 increases three orders of magnitude as the Ga content varies from 0.00 to 0.06, indicating that the localization length approximately shortens by one order of magnitude. As a result, it remarkably enhances carrier localization and increases resistivity by four orders of magnitude at 2 K shown in Fig. 2(a). Furthermore, the $S(T)$ versus $T^{1/2}$ plot at low temperatures displayed in Fig. 3(d) follows a straight line for all samples investigated, which is in good agreement with the behavior $S(T)\propto T^{1/2}$ in the limit of $T\rightarrow0$ predicted by 3D VRH model.[24] As shown in Fig. 3(d), the slope of the fitted line related to the density of states near Fermi level $N(E_F)$ decreases with increasing Ga content, suggesting that LZMGO becomes a strongly disordered system at low temperatures where states are localized.

This work was financially supported in part by the National Science Council of ROC under Grant No. NSC 96-2212-M-032-008-MY3.

[1] P. Mandal and S. Das, Phys. Rev. B **56**, 15073 (1997).
[2] S. Roy and N. Ali, J. Appl. Phys. **89**, 7425 (2001).
[3] G. T. Tan, S. Y. Dai, P. Duan, Y. L. Zhou, H. B. Lu, and Z. H. Chen, J. Appl. Phys. **93**, 5480 (2003).
[4] C. Mitra, Z. Hu, P. Raychaudhuri, S. Wirth, S. I. Csiszar, H. H. Hsieh, H.-J. Lin, C. T. Chen, and L. H. Tjeng, Phys. Rev. B **67**, 092404 (2003).
[5] S. W. Han, J.-S. Kang, K. H. Kim, J. D. Lee, J. H. Kim, S. C. Wi, C. Mitra, P. Raychaudhuri, S. Wirth, K. J. Kim, B. S. Kim, J. I. Jeong, S. K. Kwon, and B. I. Min, Phys. Rev. B **69**, 104406 (2004).
[6] K. P. Kumar, J. W. Chiou, H. M. Tsai, C. W. Pao, J. C. Jan, P. C. Hsu, D. C. Ling, F. Z. Chien, W. F. Pong, M-H. Tsai, and J. F. Lee, J. Phys.: Condens. Matter **17**, 4197 (2005).
[7] D. C. Ling, P. C. Hsu, and Z. F. Chien, J. Magn. Magn. Mater. **304**, e340 (2006).
[8] Y. Sun, X. Xu, L. Zheng, and Y. Zhang, Phys. Rev. B **60**, 12317 (1999).
[9] H. Y. Hwang, S-W. Cheong, P. G. Radaelli, M. Marezio, and B. Batlogg, Phys. Rev. Lett. **75**, 914 (1995).
[10] T. Vogt, A. K. Cheetham, R. Mahendiran, A. K. Raychaudhuri, R. Mahesh, and C. N. R. Rao, Phys. Rev. B **54**, 15303 (1996).
[11] D. Emin, Phys. Rev. Lett. **35**, 882 (1975).
[12] M. Jaime, M. B. Salamon, M. Rubinstein, R. E. Treece, J. S. Horwitz, and D. B. Chrisey, Phys. Rev. B **54**, 11914 (1996).
[13] D. Emin and T. Holstein, Ann. Phys. **53**, 439 (1969).
[14] P. Nagels, *The Hall Effect and Its Applications* (Plenum, New York, 1980), p. 253.
[15] J. M. De Teresa, K. Dörr, K. H. Müller, L. Schultz, and R. I. Chakalova, Phys. Rev. B **58**, R5928 (1998).
[16] G. J. Snyder, R. Hiskes, S. DiCarolis, M. R. Beasley, and T. H. Geballe, Phys. Rev. B **53**, 14434 (1996).
[17] J. M. De Teresa, M. R. Ibarra, J. Blasco, J. García, C. Marquina, P. A. Algarabel, Z. Arnold, K. Kamenev, C. Ritter, and R. von Helmolt, Phys. Rev. B **54**, 1187 (1996).
[18] L. Pi, L. Zheng, and Y. Zhang, Phys. Rev. B **61**, 8917 (2000).
[19] A. Banerjee, S. Pal, S. Bhattacharya, B. K. Chaudhuri, and H. D. Yang, Phys. Rev. B **64**, 104428 (2001).
[20] R. Ang, Y. P. Sun, J. Yang, X. B. Zhu, and W. H. Song, J. Appl. Phys. **100**, 073706 (2006).
[21] C. Kittel, *Quantum Theory of Solids* (Wiley, New York, 1963), p. 55.
[22] G. N. Grannemann and L. Berger, Phys. Rev. B **13**, 2072 (1976) (and references therein).
[23] N. F. Mott and E. A. Davis, *Electronic Processes in Non-Crystalline Materials* (Clarendon, Oxford, 1971).
[24] H. Overhof, Phys. Status Solidi B **67**, 709 (1975).

[This article is copyrighted as indicated in the article. Reuse of AIP content is subject to the terms at: http://scitation.aip.org/termsconditions. Downloaded to] IP: 163.13.36.187 On: Mon, 20 Oct 2014 01:56:55